High-Speed 2x25kV Traction System Model and Parallel Solver for Extensive Network Simulations

Bassam Mohamed, *Member, IEEE,* Pablo Arboleya, *Senior Member, IEEE,*
Islam El-Sayed and Cristina González-Morán, *Senior Member, IEEE*

***Abstract*---In this work, a simplified model of a 2x25kV bi-level traction power system for feeding high-speed trains is presented. A Modified Nodal Analysis (MNA) based algorithm for solving the system with and adaptive damping factor is also explained. The main novelties of this work are the inclusion of train protections (over-current) and (over-voltage) in the model and the development of the MNA solving procedure that increase the stability and the robustness of the solution process. Another important feature of the model is that can be easily adapted to a single voltage feeding systems by deactivation of specific parameters. The accuracy and performance of the proposed simulator is compared and verified relative to the derivative based solvers.**

***Index Terms*---Power Flow, Modified Nodal Analysis, Backward/Forward Swept, Newton-Raphson, Adaptive Damping Factor, Railways, Traction Power Systems, 2x25kV AC railway.**

I. Introduction

ACCORDING to the International Association of Public Transport (UITP) [1], 400 billion of trips are made each year in the European Union and 15% of those trips are made using public transport. Among the trips made using public transportation, 45% are made using railway systems. Railway transportation is recognized as the most environmental friendly form of mass transport with an average consumption of 0.12 kWh per passenger and kilometer and it is also the safest transportation system. Among all kind of railway transportation systems, high-speed railways (HSR) for connecting major cities became quite popular around the world with more than 8.9 billion of passengers each year and more than 38000km of electrification. China accounts for more than two-thirds of those kilometers and it will reach 30000km by 2020, but the degree of development of HRS is also very high in Europe (nearly 9000km) and in Japan. In other countries like United States and Australia the debate about these kind of transportation systems is already open.

In this context, the number of researchers working on this issue in the last years has grown in a significant way. Many efforts have been invested not only in the development of technologies applied to vehicles but also to the power systems that feed them and that are an essential part of the the necessary infrastructure.

Many of the works presented in the last years were devoted to study the impact of new technologies in the traction network or the impact of the traction network over the main distribution or transport grid. For instance, in [2], a methodology of optimize the off-board hybrid energy storage systems in AC rails is proposed. The same authors studied the effect of adding renewable generation inside the traction network in [3]. In [4] the traditional AC traction networks are replaced by 24kV DC traction systems using multilevel converters. [5] proposes the use of power electronic links between the neutral zones of 2x25kV AC traction systems to reduce the the losses and the investment cost and [6] develops optimization methodology to study the impact over the electrical grid of a railway corridor composed of 8 railway substations connected to the primary grid and 10 lines.

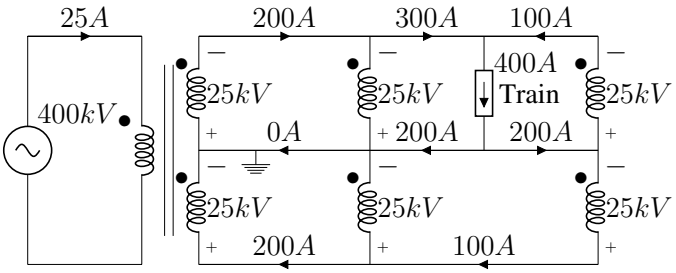

Fig. 1: 2x25kV AC traction system with two cells.

For carrying out the different studies it is crucial the development of accurate and effective mathematical models of all elements present in the infrastructure. The degree of detail of the different models varies depending on their application. In the case of power quality studies, we can find very detailed models of the electrical infrastructure and the trains. A very good examples of the integration of a detailed model of train plus high speed infrastructure are the one proposed in [7], [8], [9]. The model presented in [10] has been specifically designed for studying the problem of low frequency oscillations in traction networks.

A common feature of all of the above-mentioned models is that all of them are very complex and accurate models suitable for being used in transient simulations with a low number of lines and trains. However, they are not suitable for planning purposes with long simulation periods and a huge number of trains, lines and substations. For this kind of studies, simplified models solved using time-varying curves in quasi-static simulations are the most suitable. We can find in the literature many steady state models for DC traction systems [11], [12] and also for AC traction systems. As far as high speed systems are concerned there can be several types of feeding systems, an analysis of most of them can be found in [13]. By far the most common is called 2x25kV bi-level power system like the one represented in Fig. 1. As it can be observed, the transformer connecting the AC traction system with the main grid has the secondary winding split in two,

B. Mohamed, P. Arboleya, I. El-Sayed and C. González-Morán are with the Department of Electrical Engineering, University of Oviedo, Spain e-mail: arboleyapablo@uniovi.es

This work was partially supported by the Government of the Principality of Asturias under grant FC-15-GRUPIN14-127.

Manuscript received XXX, 2018; revised XXX, 2018.

the central point (grounded) is connected to the rails while the other two points are connected to the overhead feeding system (catenary from now on) and the return conductor. By means of autotransformers, the sections are divided in different cells. A section is fed by a power transformer and the different sections are separated by dead-zones or neutral-zones. The train is electrically connected between the catenary and the rails. With this system, the energy is transported at 50kV in the cells without trains reducing the losses and reducing the number of required substations.

This paper is going to be devoted to the development of a simplified model and quasi-static solving procedure for this kind of system, but the same model can be used for single-voltage systems just by deactivation of specific elements. It is not the first attempt or proposal to model and solve the 2x25kV networks. For instance, in [14], an equivalent monovoltage system of the classic 2x25kV system is proposed by using a Fortescue theorem. As the authors mentioned, the solution is elegant, accurate and it reduces the computation time but it is really complicated to use and it must be mentioned that it only works under the assumption that positive and negative catenaries are balanced, which could not be true in a general case. [15] used the Carson equations to model together the rails and the soil in a simplified manner. A modified current injection method for solving these kind of systems was presented in [16], and in [17], the authors used a backward /forward swept (BFS) method. In [18], the authors demonstrated that the BFS algorithm is faster than the conventional derivative based algorithms. However BFS algorithms present serious convergence problems in the presence of non-reversible substations (in case of DC systems) and other non-smooth characteristic loads/generators, like for instance, trains with over-voltage and over-current protection.

The proposed model, unlike those discussed above, considers the use of an over-current and over-voltage protection in the trains and it is specially designed for being used in massive simulations with long simulation periods and a huge number of trains and substations. The solver is based on a modified nodal analysis (MNA) algorithm with an adaptive damping factor making it much more stable and robust in terms of convergence but still much faster than those derivative based as it will be demonstrated. The paper is structured as follows. In the next section the models of the different devices present in the network are described as well as the train model and integration procedure of these devices and trains inside the network model is explained. Section III describes the solving procedure. In section IV, a set of cases of study are presented and analyzed. Finally, in section V the conclusions are stated.

II. Mathematical Model

Through the different subsections of this section we will describe the different mathematical models of the devices present in the network and the trains. Finally we will describe how to integrate all of them within the network model. For describing the different lines of the systems, a lumped model like the ones proposed in [19] and [20] are used.

To integrate all the equations in the system in a compact way, the connection matrix (Γ) described below is used repeatedly throughout the article. Γ is used to generate a linear combination from a given input vector. The element $\Gamma(m,n)$ represents the participation factor of input (n) in the output (m). The incidence matrix is a connection matrix where rows represent devices (line impedances, train, sources, ...) and columns represent nodes. All elements in Γ are cleared to zero except the elements of positive and negative nodes, that are set to 1 and -1 respectively as defined in Equation 1.

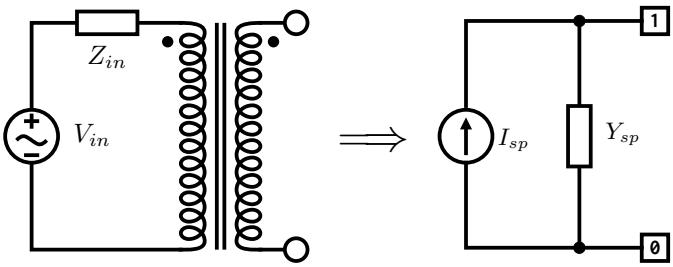

Fig. 2: Simulation model of a single supply substation

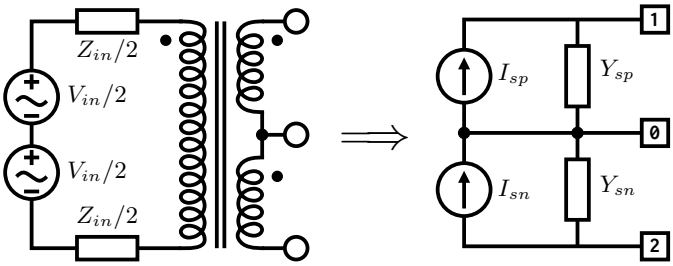

Fig. 3: Simulation model of a dual supply substation

$$\Gamma(\mathbf{m},\mathbf{n}) = \begin{cases} 1 & \mathbf{n} = \text{Positive node of device} \quad \mathbf{m} \\ -1 & \mathbf{n} = \text{Negative node of device} \quad \mathbf{m} \\ 0 & \text{otherwise} \end{cases} \quad (1)$$

The device voltage vector (V_d) and the injection current vector (I) contain respectively the voltage drop in all devices of the system and the current injected at each node. They can be calculated as a function of the nodal voltage vector(V) containing the voltage in all nodes of the system respect to ground and the device current vector (I_d) containing the current through all devices respectively by means of the incidence matrix as shown in Equation 2 and Equation 3.

$$V_d = \Gamma \times V \quad (2)$$

$$I = \Gamma^T \times I_d \quad (3)$$

A. Substation Model

The traction substations connect the traction network with the main high voltage (HV) grid. Each substation includes a power transformer to adapt the HV at primary side to traction voltage at the secondary side. In Fig. 2 and Fig. 3 (left), the electrical model of the traction substation for the single-voltage and bi-voltage cases are depicted respectively.

The high voltage side can be replaced by Thvenin equivalent circuit to simplify the model. The series impedance (Z_{in}) at the primary side of the transformer is calculated based on the short circuit power of the substation and the leakage inductance of the transformer. In the case of single feeding system, the substation model can be simplified using the Norton equivalent

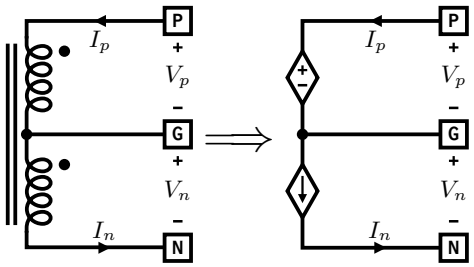

Fig. 4: Simulation model of autotransformer

circuit (current source with shunt admittance) as shown in Fig. 2 (right). The current source based model is more suitable for the MNA algorithm because it provides a direct current injection in the node. In bi-voltage feeding systems, the primary side circuit can be divided symmetrically into two voltage sources and two series impedances. Fig. 3 (right) shows the simplified model obtained using the Norton equivalent of a bi-voltage feeding system substation. The midpoint between the two circuits is used as a ground reference. The substation model for the bi-voltage system can be defined based on the following equations. We are going to refer to the no-load voltage between the terminals 1 and 0 as positive voltage (V_{sp}), and the no-load voltage between the terminals 0 and 2 as negative voltage (V_{sn}). Both voltages will be expressed in p.u. and they can be related by means of the turn ratio of their respective windings as follows:

$$V_{sn} \; = \; V_{sp} \; / \; N \tag{4}$$

The primary to positive turn ratio N_p and the primary to negative turn ratio (N_n) can be obtained using the next expressions:

$$N_p = (V_{sp} \times V_b) \; / \; V_{in} \tag{5}$$

$$N_n = (V_{sn} \times V_b) \; / \; V_{in} \tag{6}$$

Where V_b is the base voltage in (V) and V_{in} is the voltage at the HV side of the substation in (V). The admittances Y_{sp} and Y_{sn} in p.u. of the equivalent current sources (see Fig. 2 and Fig. 3 (right)) are obtained by means of the next equations:

$$Y_{sp} = Z_b \; / \; (Z_{in} \times N_p^2) \tag{7}$$

$$Y_{sn} = Z_b \; / \; (Z_{in} \times N_n^2) \tag{8}$$

Where Z_b represent the base impedance in (Ω). Using the previously defined impdances we can obtain the equivalent current sources in p.u. of the substation I_{sp} and I_{sn}.

$$I_{sp} = Y_{sp} \times V_{sp} \tag{9}$$

$$I_{sn} = Y_{sn} \times V_{sn} \tag{10}$$

We will define a vector I_c with n positions, being n the total number of nodes that will represent the nodal current injection of all constant sources. I_c will have all zeros except in the two first positions in which we will place $-I_{sp}$ and I_{sn} respectively.

B. Autotransformer Model

In bi-voltage feeding systems, the section is divided into cells. The autotransformer is placed at the end of each cell. It has two windings (positive and negative) and it is connected by three terminals (P,G and N) to the overhead feeder, the rails and the return conductor respectively (see Fig. 4 (left)). In most of the cases, the autotransformer has unity turns ratio. In asymmetrical feeding systems, the negative voltage (V_n) maybe much higher than the positive voltage (V_p) to reduce the losses of the negative feeder. The model of a ideal autotransformer can be represented using two dependent sources, a voltage and a current source as shown in Fig. 4 (right). The leakage and magnetizing impedances of the autotransformer are neglected to simplify the model. The accuracy of the solution is acceptable because those impedances are around 1%. The power transferred between the two winding through the magnetic coupling is defined in Equation 11.

$$S \; = \; I_p^* \; \times \; V_p \; = \; -I_n^* \times V_n \tag{11}$$

All autotransformers in the system can be defined by means of two linear matrix equations, the voltage equation and the current equation. In this case N will represent a diagonal matrix with all autotransformer turn ratio. The voltage relation between positive and negative ports is defined by Equation 12. Each autotransformer adds its positive current (I_p) to the unknown vector which includes also the node voltages (V). The negative current (I_n) can be substituted by the positive current (I_p) using the Equation 13.

$$V_p = \quad N \times V_n \tag{12}$$

$$I_n = -N \times I_p \tag{13}$$

The connections of autotransformers are represented by two incidence matrices. The first one (Γ_P) represents the positive winding on the top, while the connection of negative winding is represented by (Γ_N). The voltage equation of the autotransformer expressed in Equation 12 can be expressed for all the autotransformers in the system using the nodal vector and the incidence matrix as follows:

$$0 \; = \; \Gamma_p \times V \; - \; N \times \Gamma_n \times V \; = \; C \times V \tag{14}$$

Where (C) is a constant matrix $C \; = \; \Gamma_p \; - \; N \; \times \; \Gamma_n$. Equation 14 is added to the mathematical model to compensate the additional unknowns added by I_p. The nodal injection current of the autotransformer (I_a) is defined also based on the positive port current (I_p) and the transpose of the (C) matrix as shown in Equation 15.

$$I_a \; = \; \Gamma_p^T \times I_p \; - \; \Gamma_n^T \times N \times I_p \; = \; C^T \times I_p \tag{15}$$

C. Train Model

The reference power profile (P_{ref}) of the train is given as input for the simulator via a file called XTP generated by an external software containing a very detailed electro-mechanical model of the train, for each trip the XTP file contains the position, the time respect to the start of the trip and the power reference. Each profile represents a single trip of a train on a specific track which may consists of multiple of sections.

The distance of the profile data must be consistence of the total length of the track. The simulator reads the XTP data and interpolate them on a fixed step time. The train is located on its section and cell based on its position relative to the

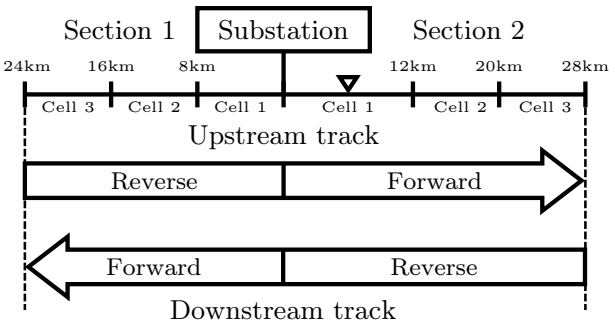

Fig. 5: Sections directions in dual track example

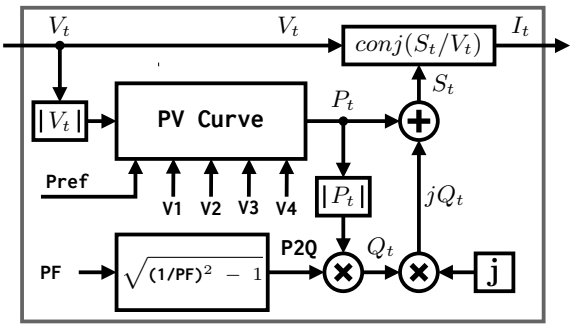

Fig. 7: Train current model based on protection curves

track. Each section may be included in different tracks with different directions. Fig. 5 shows an example of dual tracks for the same trajectory. In this case, both tracks will include the same sections but in reverse order and direction. The section is defined as forward if the train is traveling from the substation to its terminals. Otherwise the section is defined as reverse. The total length of this trajectory is 52 km divided into two sections with three cells for each one of them. Assuming, there is a train on upstream track at 30 km. This means, the train is on the first cell of the second section at 6 km from the substation. Then, the train position can be normalized relative to its cell length to be 0.5 pu.

The train is connected to the network by two nodes (positive and ground). This connection for all trains in the system is defined by the incidence matrix of the train (Γ_t). Each train is represented by single row where the column of the positive node is set to 1 and the column of the negative node is set to -1. The reference power of the train maybe limited in traction or braking mode by the over-current and over-voltage protection respectively. The over-current protection shown in Fig. 6a is activated at low voltage profile, usually when the train is in traction mode absorbing power from the catenary. If the voltage is lower than ($V2$), the train power is reduced linearly until it is blocked totally when the voltage is lower than ($V1$). Fig. 6b shows the squeeze control which protects the system from over-voltage by limiting the regenerative braking power when the voltage is higher than ($V3$). For voltages higher than ($V3$), the train can not inject any regenerated power into the catenary. The blocked power is derived and burned by the rheostatic braking system inside the train. Summarizing the train power (P_t) can be obtained as a function of the power reference (P_{ref}) and the catenary voltage as follows:

$$P_t \ = \ \texttt{PV}(V_t, Pref) \tag{16}$$

where the function **PV** represents the protection curves previously defined. The simulator calculates the reference value of the reactive power assuming specified power factor.

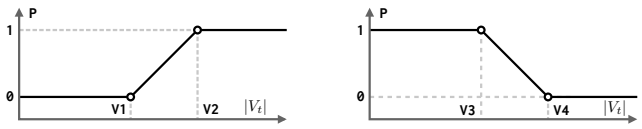

(a) Over-current protection (b) Over-voltage protection

Fig. 6: Protection curves

Equation 17 defines the ratio between active Q_t and reactive P_t power for a given power factor PF.

$$P2Q \ = \ \sqrt{(PF)^{-2} \ - \ 1} \tag{17}$$

The train reactive power can be obtained as

$$Q_t \ = \ |P_t| \ \times \ \texttt{P2Q} \tag{18}$$

The train current is updated by Equation 19 based on the complex power (S_t) and the voltage (V_t).

$$I_t \ = \ conj\left(S_t \oslash V_t\right) \tag{19}$$

Finally, a vector with all voltages between the catenary and the rails for all trains can be obtained using Equation 20 and a vector with all nodal currents injected by the train can be computed using Equation 21.

$$V_t \ = \Gamma_t \times V \tag{20}$$

$$I_{nt} = \Gamma_t^T \times I_t \tag{21}$$

Fig. 7 shows the block digram of the train model which updates the train current at each iteration of the solver.

D. Network Model

The topology of the traction network is updated dynamically based on the position of all trains at each instant. The solver will divide the nodes in static and dynamic nodes. The static nodes include the terminals of the substations and autotransformers. We define the static lines as the connections between the static nodes assuming the network without trains. The dynamic network is reconstructed at each instant considering that the trains split the static lines depending on their position. For this purpose, an optimized line splitting procedure has been designed and implemented. The line splitting procedure divides the positive (catenary) and ground feeders (rails) into lines segments. It must be pointed out that the return conductors remain always as a static lines. The 1 is used for splitting a specific line. First, trains are sorted and classified according to their position on the line from the source node. Then, trains are grouped and located at the existing static nodes or new dynamically created nodes. Finally, new dynamic lines are created for connecting the source and destination nodes with the new dynamic nodes. The distances from the source node are normalized relative to the line length so the destination node will be located always at 1. The length of line segments is limited to a minimum length (MinX) to prevent from creating

Algorithm 1 Split(Train , Line)

```
Sort(Train)
Pre = Line.Source
Dst = Line.Destination
PreX = 0
for k = 1 to Train.Count do
    X = Train.X(k)
    dx = X - PreX
    if ((1 - X) < MinX) then Train.Node(k) = Dst
    else if (dx < MinX) then Train.Node(k) = Pre
    else
        NewNode = AddNode()
        Train.Node(k) = NewNode
        AddSeg(Pre, NewNode, dx)
        Pre = NewNode
    end if
    PreX = X
end for
AddSeg(Pre, Dst, 1 - PreX)
```

ill conditioned systems. The splitting algorithm may shift the trains to nearby nodes to avoid this condition. MinX must be less than half the length of the trains to ensure the accuracy of the solution. The variable (Pre) tracks the previous node number that is initialized as the source node, while the variable (PreX) stores its location. The previous node is the starting point of all segments. The last line segment ends with the destination node, while other intermediate segments end with new nodes. The algorithm adds the last line segment in all cases even when there is no trains. An intermediate line segment is added for new node. The connection of the line segments are represented by incidence matrix (Γ_L). Fig. 8 shows different cases faced by the line splitting algorithm depending on the train positions. The following paragraphs explain the case study shown in Fig. 8.

1) Train located near the source node (T1): If the distance (X1) is less than MinX, the train is shifted to the source node.
2) Train located far from any node (T2): If the distance with the previous node (X2) is greater than MinX, the train is located at a new node. A new line segment is added to connect the previous node with the new one.
3) Train located near the previous node (T3): If the distance between the train and the previous node (dX1) is less than the MinX, the train is located at the previous node. This condition maybe also applied on the source node as special case.
4) Train located near the destination node (T4): If the distance between the train and the destination node (dX2) is less than the MinX, the splitting algorithm shifts the train to destination node.

III. Solving Procedure

It must be remarked that, as it was previously mentioned, each substation can feeds different sections that are separated from other sections fed by different substations by neutral zones without any electrical connection. The simulator solves each

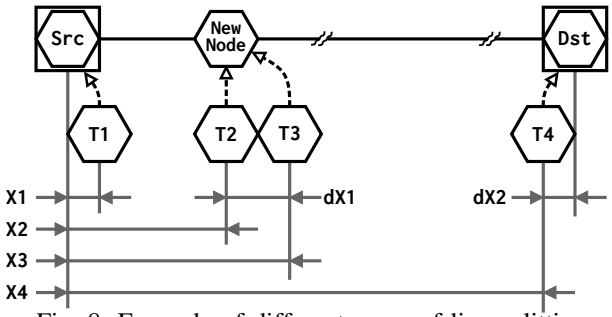

Fig. 8: Example of different cases of line splitting

network fed by an individual substation independently and in a parallel way. Taking advantage of this feature the speed of the solving procedure can be increased. In all the representations in this paper, we will assume the positive current reference when the direction of the current is to the right part of the scheme. The voltage measurements are relative to the ground node. All currents and voltages are in rms value. The mathematical model is based on the MNA as defined in Equation 22.

The unknown vector (x) includes the voltage of all nodes (V) and the current of the positive port of the autotransformer (I_p). The equations of the mathematical model are classified into two group. The first group represents the KCL at each node . The second group represents the voltage equation of the autotransformer. The nodal admittance matrix (Y_n) is used to model the constant admittance of the lines segments and shunt elements as defined in Equation 23. The (Y_n) matrix is built based on the line splitting. The (A) is constant during the all iterations of a single instant of the simulation. The vector (I_b) represents the total nodal injected current at each node which includes the constant current of the substations (I_c) and the nonlinear current of the trains (I_{nt}) as defined in Equation 22.

$$\begin{array}{ccccc} A & & \times & x & = & b \\ \left[\begin{array}{cc} Y_n & C^T \\ C & 0 \end{array}\right] & & \times & \left[\begin{array}{c} V \\ I_p \end{array}\right] & = & \left[\begin{array}{c} I_b \\ 0 \end{array}\right] \end{array} \begin{array}{l} \text{KCL} \\ \\ \text{Equation 14} \end{array} \quad (22)$$

where the nodal admittance matrix can be computed as

$$Y_n \;=\; \Gamma_L^T \times Y_L \times \Gamma_L + Y_{sh}, \quad (23)$$

Y_L is a diagonal matrix with the diagonal terms represent admittances of the lines. Y_{sh} is also a diagonal matrix with terms in the diagonal represent all shunt admittances present in the system. I_b represents all current injections of the trains as well as the constant sources of the substations, it can be calculated as

$$I_b \;=\; I_c + I_{nt} \quad (24)$$

The simulator solve this equation using LU factorization implementation of KLU linear solver [21]. KLU is specially designed to solve the linear systems generated form the mathematical models of electric circuits. At the initialization stage, the solver factorizes the (A) matrix into lower (L) and upper (U) matrices. During each iteration, the solver updates the (I_b) vector based on the nonlinear current of the trains. Then, the linear system is solved by two steps of substitutions as shown in Equation 25. The lower triangle matrix is solved

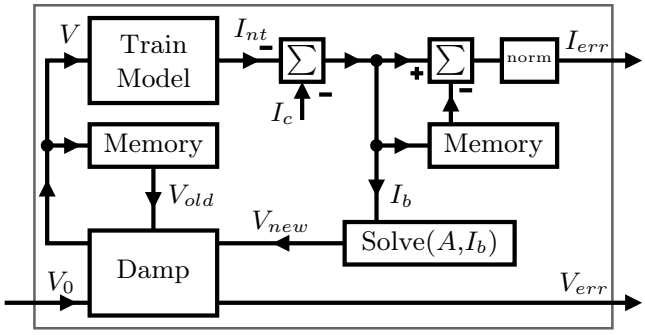

Fig. 9: Block diagram of the solver function

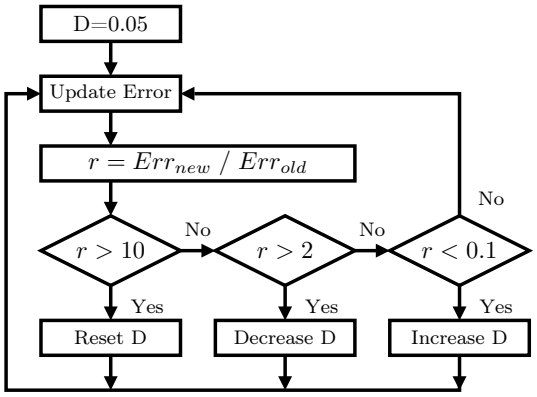

Fig. 10: Flow chart for updating the damping factor

by forward substitution, while the backward substitution is used for solving the upper triangle matrix.

$$\begin{array}{ll} A \quad \times x = b & \text{1) Solve Forward:} \quad L \times y = b \\ L \times U \times x = b & \text{2) Solve Backward:} \; U \times x = y \end{array} \tag{25}$$

For the first iteration, the nodal voltages are initialized to the substation open circuit voltage. During the iterative process (summarized in Fig. 9), the nodal voltage is updated based on the adaptive damping algorithm represented in Fig. 10 to avoid oscillations and divergence.

The damping factor (D) forces the algorithm to select an intermediate point between the old (previous iteration) and new voltage (current iteration) as defined in Equation 26. This operation is performed in the "Damp" block of Fig. 9.

$$V = D \times V_{new} + (1 \; - \; D) \times V_{old} \tag{26}$$

The Damping factor may be set to vary between 0.01 and 1. When $(D \approx 1)$, the solver jumps directly to the new voltage which may improve the speed in normal cases. However, this condition may lead to divergence in critical cases. Low values of damping factor $(D < 0.01)$ will slow down the convergence rate but the algorithm becomes more robust. The solver modifies the value of the damping factor dynamically based on the convergence rate.

The error of each iteration is estimated as a norm combination of the per unit difference error for the nodal voltage and the injection current as defined in Equation 27.

$$Err = \underbrace{\| \; V_{new} - V_{old} \; \|}_{V_{err}} + \underbrace{\| \; I_{new} - I_{old} \; \|}_{I_{err}} \tag{27}$$

First, the solver initializes the damping factor with to a low value $(D = 0.05)$ to achieve a robust convergence rate in the first iterations. Then, the solver increases the damping factor gradually when the case has a smooth convergence rate to increase the convergence speed. The damping factor is reset to the initial value if the solver detects any overshot or oscillation of the error. Equation 28 defines the convergence rate (r) as a ratio between the errors of successive iterations.

$$r = \frac{Err_{new}}{Err_{old}} \tag{28}$$

The numerical limits shown in the flow chart of Fig. 10 are used to avoid overshooting and oscillation. Similar strategies have been applied to derivative based methods. For example, Levenberg-Marquardt method is known as damped least square method which is widely used for solving the nonlinear systems of equations [22], [23], [24]. However, it is not designed to deal with non-smooth characteristics like the ones introduced by protection curves of the trains. In the following section, the performance of the proposed algorithm is compared with an improved version of the Levenberg-Marquardt algorithm.

IV. Cases of Study

A. Test case of single section

Fig. 11 shows a simple network configuration of a single section with three cells and two parallel catenaries that share the same autotransformers and return conductor. The rails of the two tracks are electrically connected so it can be considered as an equivalent rail. The impedance parameters of this test case are listed on Table I based on the reference [19]. Two trains from both terminals are launched when the simulation start fed by one catenary. After 25s, another train departs from the substation located at the left part of the representation and fed by the second catenary. The simulation represents 200s. In the printed version of this manuscript is represented the instant t=101s. However, the electronic version include the 200 cases. It is possible to interact with the graphical representation and select any of the 200 instants by means of the controls placed at the bottom of the figure.

In this case, the power profiles of all trains are generated by repeating patterns of acceleration and deceleration with intervals of constant power between them. In Fig. 12, the trains (T1,T2 and T3) position, power, real and imaginary current, catenary voltage drop from the substation to the train and catenary voltage are represented. The peak power of the trains is selected between 10 MW for acceleration and 4 MW for braking. The power factor has been set to 0.9 (lagging) for the whole simulation but it could be defined as a complex function depending on the active power reference. The actual power of the train is following the same reference profile because the train voltage does not activate the protection curve most of the time. The real and imaginary components of the

TABLE I: Impedance configuration of the test cases [19]

Z	R	L
Z_{in}	1 Ω	150 mH
Z_P	40 mΩ/km	0.43 mH/km
Z_G	23 mΩ/km	0.22 mH/km
Z_N	54 mΩ/km	0.63 mH/km

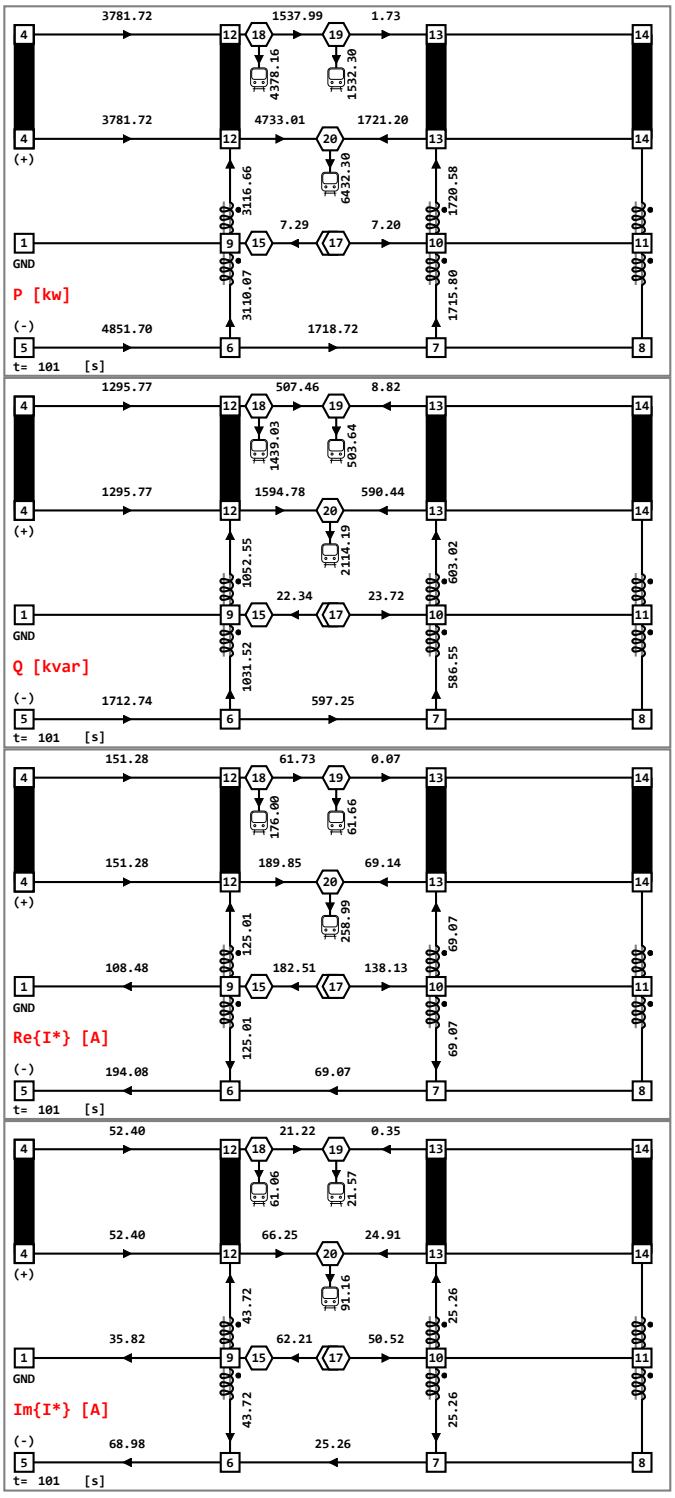

Fig. 11: Topology of AC traction network

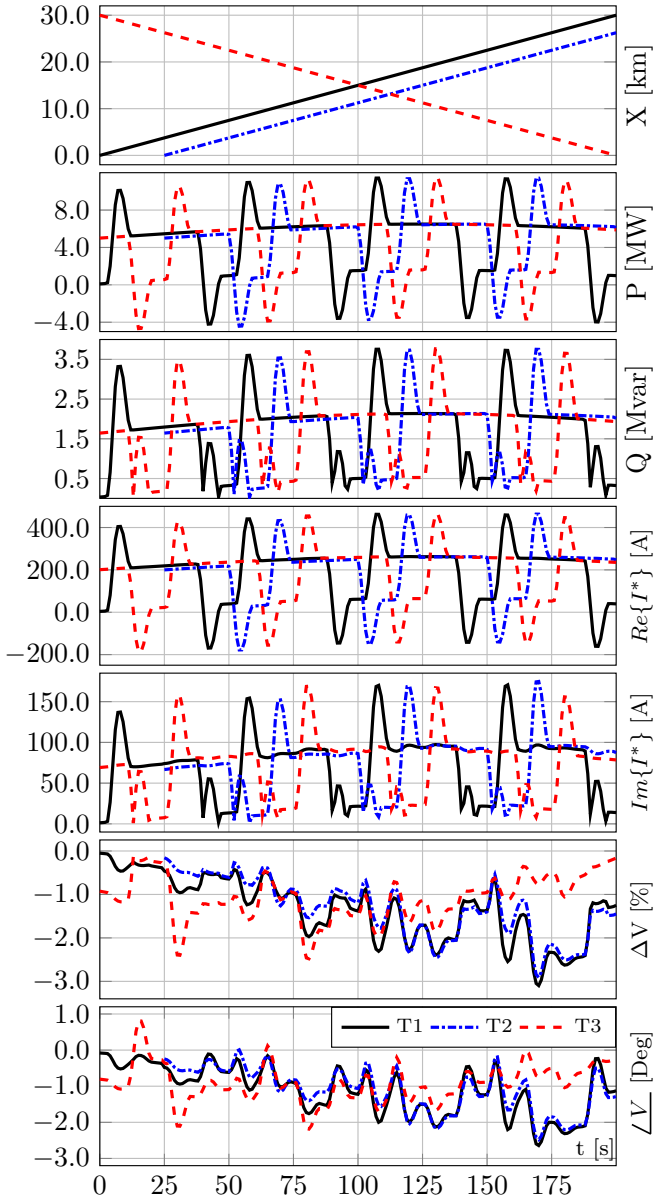

Fig. 12: The simulation results of the three trains test

train conjugate current are represented in Fig. 12, the obtained profiles are highly correlated to the active and reactive power of the train.

The voltage deviation (ΔV) is less than 3% in all cases. Even when the first and second trains (T1 and T2) are separated by a fixed distance of 3750m, they have a similar voltage profiles because they share the same catenary and the voltage drop is limited to 3%. At the instant t=90s, both second and the third trains (T2 and T3) have similar distance relative to the start of the section and almost the same power reference, but the voltage drop is different because they are running on different catenaries. The improvement of the voltage profile due to the autotransformer can be seen when the train passes at distances of 10 km, 20 km and 30 km. The minimum voltage is caused by a peak demand power of 9 MW from the third train while the other two trains consume 5 MW.

B. Performance test

The proposed method is tested using a computer generated network which includes 10 substations feeding a track of 1000 km divided into 20 sections of 50 km as shown in Fig. 13. Each section includes two catenaries and 5 cells of the same length and the same configuration as the one represented in Fig. 11 (two independent catenaries sharing the autotransformers

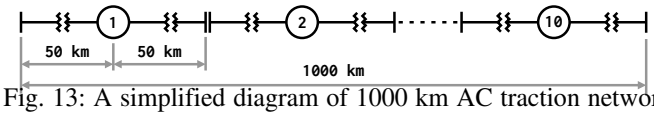

Fig. 13: A simplified diagram of 1000 km AC traction network

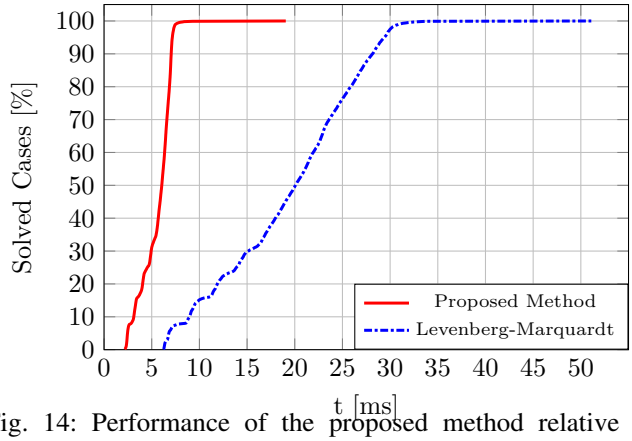

Fig. 14: Performance of the proposed method relative to Levenberg-Marquardt

and the return conductor with the rails electrically connected). A train is launched every ten minutes from both ends and the simulation period is set to 5 hours solving a case each second.

Fig. 14 compares the performance of the proposed solver relative to LM (Levenberg-Marquardt) method based on the percent of solved cases within a time out per case. The proposed method is able to solve all cases in less than 20ms per case while LM requires more than 50ms. Within a time of 10ms per case, the proposed method solve more than 99.9% of the cases while LM can solve only 15% of them. The proposed method improves the solver speed by more than 3 times relative to LM method.

V. Conclusion

A simplified model for solving AC traction systems was presented in this paper, the model has been specifically designed for being used with bi-voltage high-speed traction system but can be also adapted for solving single-voltage AC systems. The solving procedure based on Modified Nodal Analysis is faster than the derivative based solvers reaching the same level of accuracy. The implementation of the adaptive damping factor makes the algorithm very robust also in the presence of non-linear and non-smooth characteristics like the ones that the over-voltage and over-current protection of the trains add to the system.

References

[1] UITP International Association of Public Transport, from the French: LUnion internationale des transports publics, *http://www.uitp.org/*, Belgium, Europe, Founded in, 1885.

[2] S. de la Torre, A. J. Snchez-Racero, J. A. Aguado, M. Reyes, and O. Martnez, ''Optimal sizing of energy storage for regenerative braking in electric railway systems,'' *IEEE Transactions on Power Systems*, vol. 30, no. 3, pp. 1492--1500, May 2015.

[3] J. A. Aguado, A. J. S. Racero, and S. de la Torre, ''Optimal operation of electric railways with renewable energy and electric storage systems,'' *IEEE Transactions on Smart Grid*, vol. 9, no. 2, pp. 993--1001, 3 2018.

[4] A. Gomez-Exposito, J. M. Mauricio, and J. M. Maza-Ortega, ''VSC-based MVDC railway electrification system,'' *IEEE Transactions on Power Delivery*, vol. 29, no. 1, pp. 422--431, 2 2014.

[5] E. Pilo, S. K. Mazumder, and I. Gonzlez-Franco, ''Smart electrical infrastructure for ac-fed railways with neutral zones,'' *IEEE Transactions on Intelligent Transportation Systems*, vol. 16, no. 2, pp. 642--652, 4 2015.

[6] Y. Sun, Z. Li, W. Tian, and M. Shahidehpour, ''A lagrangian decomposition approach to energy storage transportation scheduling in power systems,'' *IEEE Transactions on Power Systems*, vol. 31, no. 6, pp. 4348--4356, Nov 2016.

[7] H. Hu, Z. He, K. Wang, X. Ma, and S. Gao, ''Power-quality impact assessment for high-speed railway associated with high-speed trains using train timetable - part ii: Verifications, estimations and applications,'' *IEEE Transactions on Power Delivery*, vol. 31, no. 4, pp. 1482--1492, Aug 2016.

[8] H. Hu, Z. He, X. Li, K. Wang, and S. Gao, ''Power-quality impact assessment for high-speed railway associated with high-speed trains using train timetable - part i: Methodology and modeling,'' *IEEE Transactions on Power Delivery*, vol. 31, no. 2, pp. 693--703, April 2016.

[9] M. Brenna, F. Foiadelli, and D. Zaninelli, ''Electromagnetic model of high speed railway lines for power quality studies,'' *IEEE Transactions on Power Systems*, vol. 25, no. 3, pp. 1301--1308, Aug 2010.

[10] Z. Liu, Z. Geng, and X. Hu, ''An approach to suppress low frequency oscillation in the traction network of high-speed railway using passivity-based control,'' *IEEE Transactions on Power Systems*, vol. 33, no. 4, pp. 3909--3918, July 2018.

[11] R. A. Jabr and I. Dafi, ''Solution of dc railway traction power flow systems including limited network receptivity,'' *IEEE Transactions on Power Systems*, vol. 33, no. 1, pp. 962--969, Jan 2018.

[12] P. Arboleya, B. Mohamed, and I. El-Sayed, ''Dc railway simulation including controllable power electronic and energy storage devices,'' *IEEE Transactions on Power Systems*, pp. 1--1, 2018.

[13] Y. Chen, R. White, T. Fella, S. Hillmansen, and P. Weston, ''Multi-conductor model for ac railway train simulation,'' *IET Electrical Systems in Transportation*, vol. 6, no. 2, pp. 67--75, 2016.

[14] E. Pilo, L. Rouco, A. Fernandez, and L. Abrahamsson, ''A monovoltage equivalent model of bi-voltage autotransformer-based electrical systems in railways,'' *IEEE Transactions on Power Delivery*, vol. 27, no. 2, pp. 699--708, 4 2012.

[15] M. Ceraolo, ''Modeling and simulation of ac railway electric supply lines including ground return,'' *IEEE Transactions on Transportation Electrification*, vol. 4, no. 1, pp. 202--210, 3 2018.

[16] B. Mohamed, P. Arboleya, and M. Plakhova, ''Current injection based power flow algorithm for bilevel 2x25kv railway systems,'' in *2016 IEEE Power and Energy Society General Meeting (PESGM)*. IEEE, 7 2016.

[17] S. V. Raygani, A. Tahavorgar, S. S. Fazel, and B. Moaveni, ''Load flow analysis and future development study for an ac electric railway,'' *IET Electrical Systems in Transportation*, vol. 2, no. 3, pp. 139--147, 9 2012.

[18] B. Mohamed, P. Arboleya, and C. Gonzlez-Morn, ''Modified current injection method for power flow analysis in heavy-meshed dc railway networks with nonreversible substations,'' *IEEE Transactions on Vehicular Technology*, vol. 66, no. 9, pp. 7688--7696, Sept 2017.

[19] A. Mariscotti, P. Pozzobon, and M. Vanti, ''Simplified modeling of 2x 25-kv at railway system for the solution of low frequency and large-scale problems,'' *IEEE Transactions on Power Delivery*, vol. 22, no. 1, pp. 296--301, Jan. 2007.

[20] M. Brenna and F. Foiadelli, ''Sensitivity analysis of the constructive parameters for the 2 x 25-kv high-speed railway lines planning,'' *IEEE Transactions on Power Delivery*, vol. 25, no. 3, pp. 1923--1931, 7 2010.

[21] T. A. Davis and E. Palamadai Natarajan, ''Algorithm 907: Klu, a direct sparse solver for circuit simulation problems,'' *ACM Trans. Math. Softw.*, vol. 37, no. 3, pp. 36:1--36:17, 9 2010.

[22] K. Levenberg, ''A method for the solution of certain non-linear problems in least squares,'' *Quarterly of applied mathematics*, vol. 2, no. 2, pp. 164--168, 1944.

[23] M. L. A. Lourakis and A. A. Argyros, ''Is levenberg-marquardt the most efficient optimization algorithm for implementing bundle adjustment?'' in *Tenth IEEE International Conference on Computer Vision (ICCV'05) Volume 1*, vol. 2, Oct. 2005, pp. 1526--1531 Vol. 2.

[24] P. J. Lagace, M. H. Vuong, and I. Kamwa, ''Improving power flow convergence by newton raphson with a levenberg-marquardt method,'' in *2008 IEEE Power and Energy Society General Meeting - Conversion and Delivery of Electrical Energy in the 21st Century*, Jul. 2008, pp. 1--6.